COBEM 2025
28TH INTERNATIONAL CONGRESS OF MECHANICAL ENGINEERING
ABCM Brazilian Society of Mechanical Sciences and Engineering
28th ABCM International Congress of Mechanical Engineering
November 09-11, 2025, Curitiba-PR, Brazil

COB-2025-1034
EXPERIMENTAL CHARACTERIZATION OF A SMALL-SCALE REFRIGERATION MACHINE OPERATING WITH CO_2 IN A TRANSCRITICAL CYCLE

Guilherme de Moraes Ramiro, guiramiro2003@ufmg.br[1]
Gabriel Henrique de Paula Ferreira, gabrielhpf@ufmg.br[2]
Bruno Clayton de Paula Ferreira, brunocpf@ufmg.br[1]
Erick Drummond Martins, erick-dru@ufmg.br[1]
Willian Moreira Duarte, willian@demec.ufmg.br[2]
Antônio Augusto Torres Maia, aamaia@ufmg.br[2]
[1] Undergraduate Program in Mechanical Engineering at the Federal University of Minas Gerais, Av. Antônio Carlos, 6627, Pampulha - Belo Horizonte - MG - CEP 31270-901
[2] Graduate Program in Mechanical Engineering at the Federal University of Minas Gerais

Abstract. *Given the increasing importance of environmentally friendly refrigerants, there is a significant gap in research regarding the use of these substances in a sustainable context. These refrigerants must exhibit favorable thermodynamic properties while maintaining a low environmental impact, complying with international regulations aimed at reducing emissions of substances that contribute to global warming and ozone layer depletion. CO_2, in particular, stands out as a viable alternative due to its low global warming potential (GWP), availability, and status as a natural fluid that does not harm the ozone layer. The experimental characterization of refrigeration systems operating with CO_2 in a transcritical cycle is essential to advancing the understanding of such systems, especially on a small scale. The main objective of this study is to conduct an experimental characterization of a small-capacity refrigeration machine operating with CO_2 under different steady-state operating conditions. In this regard, the study aims to evaluate system performance, identify improvement opportunities, and provide data for validating mathematical models. To achieve this, detailed measurements of parameters such as pressure, temperature, flow rate, and energy consumption will be carried out, enabling a comprehensive analysis of the system's behavior. The results indicated that gas cooler pressure has the greatest influence on the system performance, with an optimal operating range observed around 80 bar. At this condition, the system reached a maximum cooling capacity of 1250 W, a gas cooler heat rejection rate of 1800 W, and a coefficient of performance (COP) of 2.7. The compressor's volumetric efficiency also peaked near this range, reaching approximately 71%. The collected data demonstrate the feasibility of using CO_2-based small-scale refrigeration systems and provide input for mathematical modeling and future energy optimization strategies, contributing to the advancement of more efficient and sustainable technologies.*

Keywords: *Sustainable Refrigeration, Natural Refrigerants, Carbon Dioxide, Transcritical Cycle, Experimental Characterization, Small-Scale Refrigeration System, Energy Efficiency*

1. INTRODUCTION

Environmental problems, such as climate change, are leading to a significant increase in planetary temperatures (Climate Reanalyzer, 2024). With this temperature rise, energy consumption in refrigeration and air-conditioning systems increases, resulting in continuous growth of greenhouse gas (GHG) emissions and worsening global warming (Oruç et al., 2024). The rising average temperature of the Earth has accelerated polar ice cap melting and sea-level rise due to higher concentrations of greenhouse gases in the atmosphere (IPCC, 2007). In this context, the Kyoto Protocol established targets for reducing GHG emissions (United Nations, 1997). Consequently, research has been developed to replace refrigerants with high global warming potential (GWP) and ozone depletion potential (ODP), seeking more sustainable alternatives.

In this scenario, carbon dioxide (CO_2) emerges as a promising fluid to replace synthetic refrigerants with high ODP and GWP, as it has zero ODP and a GWP of 1 (Yadav et al., 2022). Furthermore, CO_2 is economically more advantageous than other refrigerants, with a per-kilogram cost up to 65% lower compared to synthetic alternatives (Deng et al., 2025). Its thermodynamic properties are also favorable for refrigeration systems, including low compression ratio, non-toxicity, non-flammability, and natural abundance (Lorentzen, 1994). However, due to its low critical temperature (31.1°C), systems using CO_2 typically operate in transcritical cycles, especially in environments with high heat rejection temperatures (Guruchethan et al., 2023). In such cases, CO_2 demonstrates the capability to operate in the transcritical zone, where heat dissipation occurs above the critical point (at high pressures) and heat absorption takes place below the

critical point. This characteristic requires specific designs but maintains CO_2 as a technically viable and environmentally sustainable alternative.

Compact refrigeration systems have gained relevance due to the growth of residential and commercial applications, such as small-capacity heat pumps and air-conditioning units (Cao et al., 2019), as well as supermarket refrigeration systems for food preservation (Lykas et al., 2022). However, implementing sustainable technologies at this scale faces additional technical challenges, particularly regarding precise control and proper component sizing. Although demand for these systems continues to rise, there remains a significant lack of experimental studies specifically dedicated to small-scale units (Song et al., 2022), limiting progress in optimizing their energy and environmental performance. It is worth noting that, considering the substantial number of such units operating in the market, representing a considerable share of global energy consumption, developing efficient solutions for compact systems has become crucial for driving large-scale sustainability and reducing the environmental impact of the refrigeration sector.

Given these facts, the objective of this work is the experimental characterization of a small-scale refrigeration machine operating with CO_2 in a transcritical cycle. The experimental characterization in this study will focus on measuring critical operational variables such as temperatures and pressures at various points in the cycle, refrigerant flow rate, and system energy consumption, as well as efficiency parameters like the Coefficient of Performance (COP) and the compressor volumetric efficiency. Thus, we aim to verify the feasibility of utilizing this smaller-scale refrigeration system configuration, enabling its application in industries and households. Based on this, optimization strategies can be developed to improve energy performance and reduce the environmental impact of traditional refrigeration systems.

2. METHODOLOGY

2.1. Experimental Apparatus and Setup

The test bench used in this work consists of a refrigeration system operating with CO_2 in a transcritical cycle, as shown in Figure 1. This system features two spiral countercurrent flow heat exchangers with concentric tubes (evaporator and gas cooler). In both components, CO_2 flows through the innermost tube and exchanges heat exclusively with water flowing in the outermost tube. The evaporator has a length of 12.9 m and an outer diameter of 690 mm, while the gas cooler is longer at approximately 20.6 m with a diameter of 610 mm. Both heat exchangers are thermally insulated from the environment.

The expansion mechanism used is an Electronic Expansion Valve (EEV) developed by the Laboratory of Automation and Control at the Federal University of Minas Gerais (UFMG). It consists of a Swagelok SS-31RS4 micrometric valve, actuated by a NEMA-17 stepper motor, which in turn is controlled by a PID system (Martins et al., 2024), which will maintain constant superheat temperature throughout the tests.

For the primary fluid (CO_2) compressor, a compact hermetic reciprocating compressor (model SRcACB, n°6457) designed for transcritical CO_2 refrigeration systems was used, featuring 1.75 cm³ displacement and operation up to 90.7 bar discharge pressure. To prevent excessive liquid from entering the compression system, which could potentially damage the equipment, a gas-liquid separator was installed upstream of the compressor inlet, ensuring enhanced operational safety. Additionally, an oil separator was installed at the compressor outlet to prevent equipment oil from being entrained with the compressed CO_2 into the heat exchanger.

Figure 1. Photo of the refrigeration machine used.

In an experimental characterization project, acquiring maximum data is essential. Therefore, 11 T-type thermocouples were installed throughout the setup to monitor temperatures at all critical points. For flow monitoring, two SBG232

sensors were installed on the heat exchangers. These sensors have a measuring range of 0.3 to 15 l/min and an uncertainty of ±4% of the measured value plus ±1% of the final value of the measuring range. Additionally, two PN3071 pressure sensors were positioned to track the primary fluid pressure at the gas cooler (high pressure) and evaporator (low pressure). According to the manufacturer, these sensors have a measuring range of 0 to 250 bar, with an uncertainty of ±0.5% of the span. All data is recorded by a NOVUS data logger and displayed in real-time on a monitor, enabling precise machine control during operation. Figure 2 presents a diagram detailing the refrigeration system used.

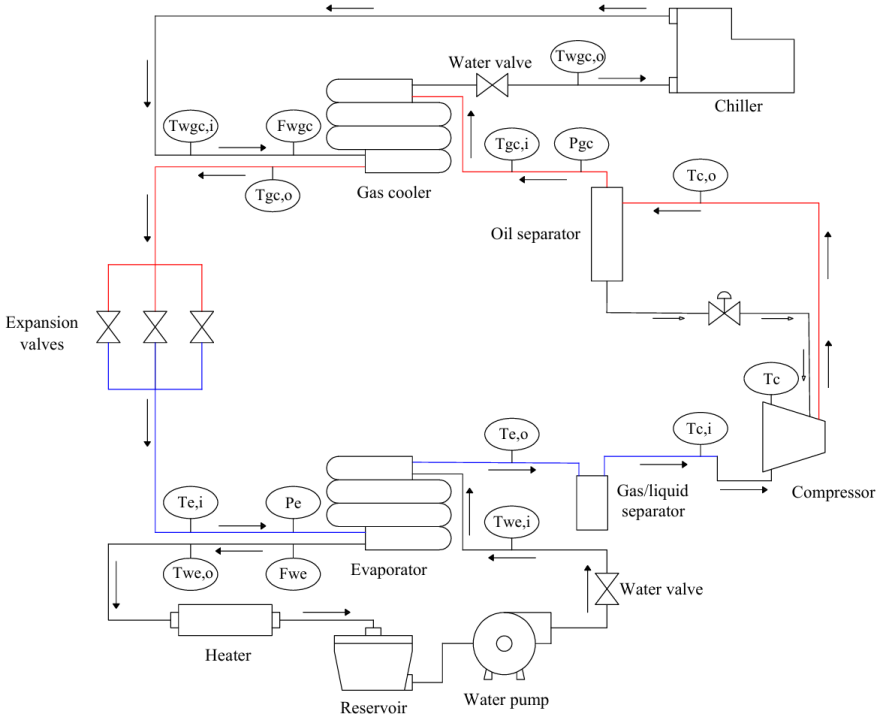

Figure 2. Refrigeration machine diagram.

2.2. Test description

The experimental campaign was designed to systematically evaluate the transcritical CO_2 refrigeration system's performance under controlled operating conditions. Initially, the secondary fluid inlet temperature at the evaporator stabilized at a fixed setpoint of 17°C. Throughout all tests, a constant superheat of 7°C was maintained at the evaporator outlet via real-time PID control of the EEV. Simultaneously, the gas cooler pressure was systematically varied from near the critical pressure of CO_2, about 74 bar, to approximately 93.4 bar gauge. This pressure modulation was achieved by adjusting the opening of the electronic expansion valve (EEV) and regulating the secondary fluid flow rates at the heat exchangers.

At each pressure step, the system was allowed to stabilize for five minutes until stringent steady-state criteria were met: temperature fluctuations remained within ±1°C and pressure drift did not exceed ±1 bar over the interval. Upon confirming the steady-state, critical parameters, including temperatures, pressures, and refrigerant flow rates, were recorded at 1 Hz for 30 seconds. This protocol was repeated across pressure levels of 74.7, 76, 80, 82.6, 84.5, 86.6, 92, and 93.4 bar. The pressure levels were selected pragmatically, focusing solely on operational attainability and stability at readily achievable setpoints, without employing analytical parameter optimization. Table 2 presents, in summary form, the testing methodology of this work.

Table 1. Testing methodology summary.

Variable	Test Range/Levels	Control Method
Evaporator Temperature	17°C (±0.5°C)	Flow rate
Gas Cooler Pressure	74.7 to 93.4 bar (±0.5 bar)	EEV + flow rate
Superheat	7°C (±0.5°C)	PID-controlled EEV

2.3. Calculation Methods

Based on the collected experimental data, including pressures, temperatures, and secondary fluid flow rates, the main thermodynamic cycle parameters were determined, such as the Coefficient of Performance (COP), the thermal powers exchanged in the evaporator and gas cooler, and the carbon dioxide mass flow rate. To assist in the calculations, a program developed in the Python language was utilized. This program automated part of the data processing, particularly in obtaining CO_2 thermophysical properties and performing energy balances.

To calculate the refrigerant mass flow rate, an energy balance was performed on the evaporator, assuming that all energy transferred from the water (secondary fluid) to the CO_2 corresponds to the energy absorbed by the refrigerant as heat – a valid consideration enabled by the thermal insulation isolating the heat exchanger from the environment. Thus, Eq. 1 presents the method used to calculate the primary fluid mass flow rate.

$$\dot{m}_{\mathrm{CO_2}} = \frac{\dot{m}_{water} \times c_{p,water} \times (T_{in,water} - T_{out,water})}{h_{out,\mathrm{CO_2}evap} - h_{in,\mathrm{CO_2}evap}} \tag{1}$$

In Equation 1, the CO_2 mass flow rate, $\dot{m}_{\mathrm{CO_2}}$, is calculated as the heat released by the water in the evaporator – expressed in terms of the water mass flow rate ($\dot{m}_{water}$), specific heat of water ($c_{p,water}$), and the water temperature difference at the heat exchanger inlet ($T_{in,water}$) and outlet ($T_{out,water}$) – divided by the enthalpy difference of the primary fluid at the evaporator outlet ($h_{out,\mathrm{CO_2}evap}$) and inlet ($h_{in,\mathrm{CO_2}evap}$).

From this mass flow rate, the heat transfer rate of the fluid in the evaporator and gas cooler can be calculated. As seen in Eq. 1, the refrigeration capacity of the fluid is defined as the product of the mass flow rate and the enthalpy difference between the outlet and inlet of the evaporator. For the gas cooler, the calculation is similar, where $h_{in,\mathrm{CO_2}gc}$ is the enthalpy of the fluid at the gas cooler inlet, and $h_{out,\mathrm{CO_2}gc}$, is the enthalpy at the gas cooler outlet. Equation 2 presents the calculation of the heat transfer rate exchanged by carbon dioxide in the gas cooler.

$$\dot{Q}_{gc} = \dot{m}_{\mathrm{CO_2}}(h_{in,\mathrm{CO_2}gc} - h_{out,\mathrm{CO_2}gc}) \tag{2}$$

As the fluid releases heat in the gas cooler, $\dot{Q}_{gc}$ would inherently assume a negative value. However, the direction of heat transfer was disregarded since the focus lies solely on the numerical magnitude of heat rejected by the fluid in this stage. Thus, Equation 2 incorporates a multiplicative factor of (−1) to express this quantity as a positive value.

One of the key parameters studied in this characterization is the Coefficient of Performance (COP). The COP can be defined as the ratio of useful heat transferred by the system to the work it consumes, representing a performance metric for thermal machines. For the system in this work, operating as a refrigerator, the COP is specified as the ratio between the heat absorption rate by CO_2 in the evaporator ($\dot{Q}_{evap}$) – where cooling of the secondary fluid occurs – and the total power consumed by the compressor (W_{comp}). Expressing these rates in terms of enthalpy changes and considering identical mass flow rates for both terms yield the relationship presented in Equation 3.

$$COP = \frac{h_{out,\mathrm{CO_2}evap} - h_{in,\mathrm{CO_2}evap}}{h_{out,\mathrm{CO_2}comp} - h_{in,\mathrm{CO_2}comp}} \tag{3}$$

In this equation, the new terms $h_{out,\mathrm{CO_2}comp}$ and $h_{in,\mathrm{CO_2}comp}$ refer to the enthalpy of CO_2 at the compressor outlet and inlet, respectively. However, since the fluid enthalpy at the evaporator outlet equals that at the compressor inlet (identical state point), Eq. 3 can be reformulated as Eq. 4.

$$COP = \frac{h_{out,\mathrm{CO_2}evap} - h_{in,\mathrm{CO_2}evap}}{h_{out,\mathrm{CO_2}comp} - h_{out,\mathrm{CO_2}evap}} \tag{4}$$

Finally, the last parameter to be analyzed is the volumetric efficiency of the compressor, η_v. This value indicates how efficiently the compressor admits the fluid to be compressed. It is represented as the ratio between the amount of fluid that the compressor compresses and the amount it would theoretically be capable of compressing. Thus, Eq. 5 presents the calculation of this parameter, where N is the rotational speed of the compressor, $\rho_{\mathrm{CO_2}}$ is the specific density of CO_2 at the compressor inlet, and V is the displacement volume of the compressor. In the case of this system's compressor, according to the manufacturer, the rotational speed is 3510 rpm (or 58.5 Hz), and the displacement volume is 1.75 cm³.

$$\eta_v = \frac{\dot{m}_{\mathrm{CO_2}}}{N \rho_{\mathrm{CO_2}} V} \tag{5}$$

3. RESULTS

The tests were conducted according to the methodology described in Section 2.2. The subsequent analysis focuses on the impact of gas cooler pressure variation on the system's key performance parameters. During the trials, the gas cooler pressure was systematically adjusted to eight distinct levels, ranging from 74.7 bar to 93.4 bar, while the secondary fluid inlet temperature at the evaporator was controlled at 17°C (±0.5°C) and the superheat at the evaporator outlet was maintained constant at 7°C (±0.5°C) through PID control of the electronic expansion valve. Figure 3 shows the pressure curve during the test at 93.7 bar. As observed, the system maintained constant evaporator and gas cooler pressures throughout the entire experiment.

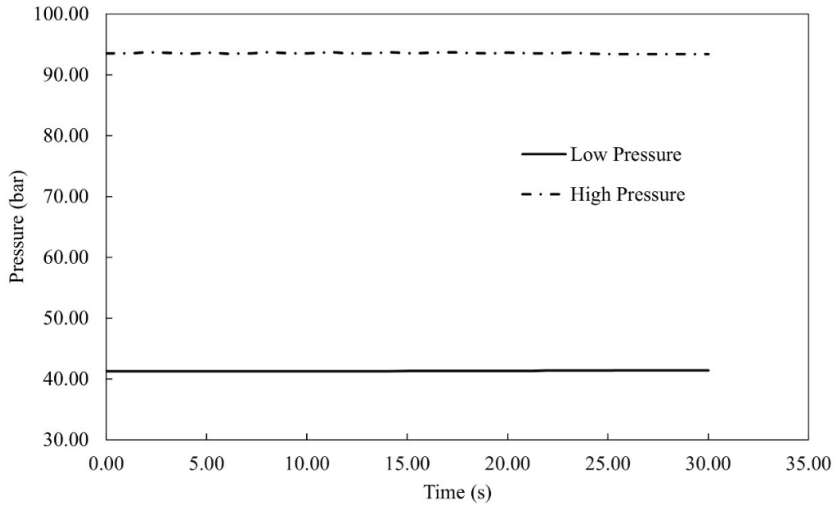

Figure 3. Pressure curves for test at 93.7 bar.

To enable the calculations outlined in Section 2.3, temperature data throughout the tests is equally critical. Accordingly, Figure 4 presents temperature values from all 11 thermocouples installed in the machine. In this figure, consistent stability is observed in the temperature readings – mirroring the pressure data trends – indicating proper operation of the electronic expansion valve.

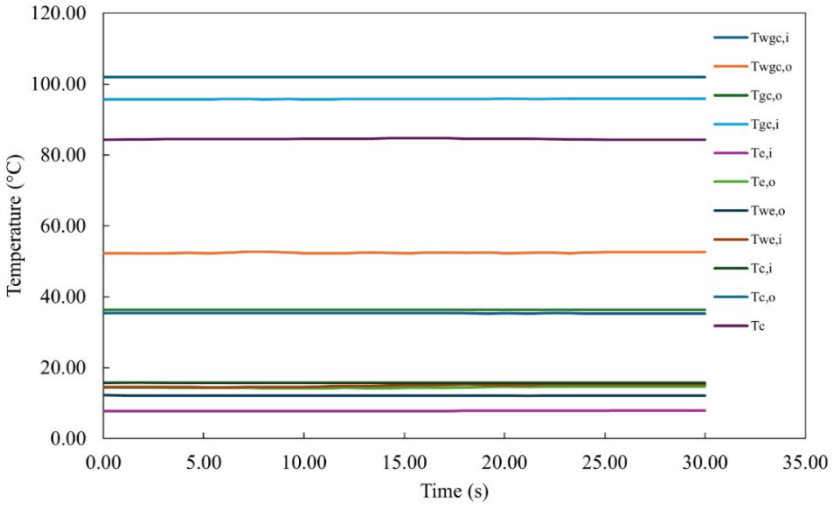

Figure 4. Temperature curves for test at 93.7 bar.

The peak temperature of approximately 102°C was recorded at the compressor discharge thermocouple (Tc,i) during the highest gas cooler pressure test (93.4 bar) – the most demanding operational condition where compressor thermal loading reaches its maximum. Despite this elevated value, the measurement remains 18°C below the manufacturer's specified 120°C maximum operating limit.

Finally, with the acquired pressure and temperature measurements – combined with the consideration of isenthalpic expansion occurring at the expansion valve – all necessary enthalpy values for subsequent calculations were determined using thermodynamic tables for CO_2.

To advance the characterization, the water flow rate data curves obtained from the SBG232 sensors must be plotted. As established in Eq.1 and 2, these data are fundamental for determining both the fluid mass flow rate and the heat rejection rate in the gas cooler. Accordingly, Figure 5 presents the flow rate profiles from the two flow sensors installed in the system.

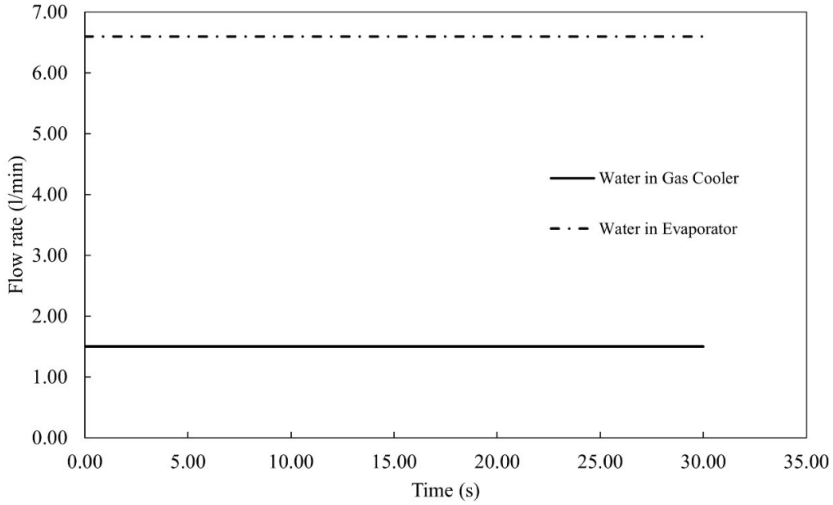

Figure 5. Water flow rate curves for test at 93.7 bar

After obtaining all the sensor curves, as shown above, it is possible to proceed with the calculation of the mass flow parameters. Using Eq. 1, the CO_2 mass flow rates for each test were determined, and the results are presented in Figure 6.

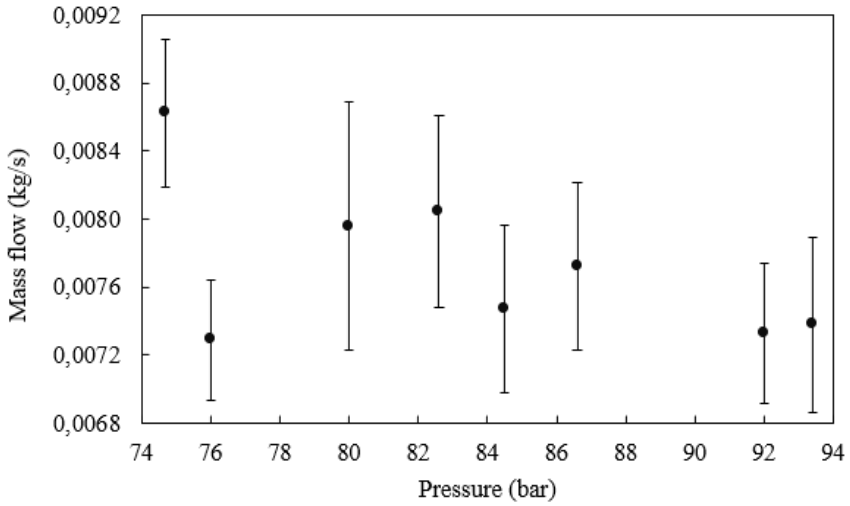

Figure 6. CO_2 mass flow rate for each test.

By analyzing the curve in Figure 6, where a non-linear behavior of the CO_2 mass flow rate can be observed throughout the tests, with an average measurement uncertainty of 6%. At first, there is a sharp drop in flow rate, from 0.0086 kg/s to around 0.0072 kg/s, which may indicate a sudden change in the fluid density or, probably, due to a change in the expansion valve opening. From pressures near 76 bar, the flow rate tends to increase again, reaching a peak of approximately 0.0081 kg/s at 82.6 bar. Between 82.6 and 84 bar, the flow rate drops again, although less abruptly than the first drop. Next, the system presents a flow rate of 0.0077 kg/s around 87 bar. Thus, it can be observed that the variation between peaks and valleys becomes smaller as the gas cooler pressure increases. Furthermore, from 87 bar onwards, the system shows a smooth and continuous decline.

With the mass flow rates previously obtained, the next step was to calculate the heat transfer rates of CO_2 in the heat exchangers. Figure 7 presents the heat exchanged between the fluid and the water in the gas cooler, calculated using Eq. 2. This value is particularly relevant for applications where the system operates as a heat pump or for conducting energy balances beyond the evaporator.

In addition, Figure 8 shows the cooling capacity of the system, which corresponds to the thermal energy absorbed by the CO_2 in the evaporator. This parameter is essential for evaluating the system's performance in refrigeration mode and assessing its ability to meet cooling demands under varying operating conditions.

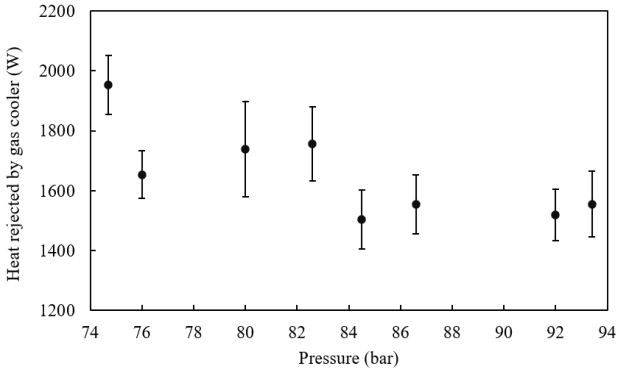

Figure 7. Heat exchanged in Gas Cooler for each test.

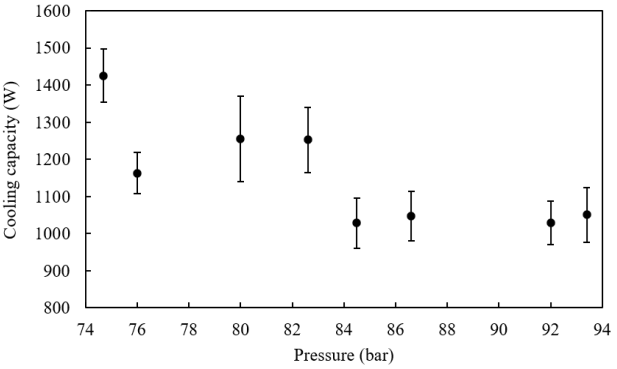

Figure 8. Cooling capacity for each test.

By analyzing Figure 7, a sharp drop in the heat transfer rate in the gas cooler can be observed — the initial value of 1950 W quickly falls to around 1650 W at pressures near 76 bar. This behavior aligns with the mass flow rate curve, as there is a direct relationship between the two parameters, as shown in Eq. 2. Then, a gradual recovery occurs until the curve reaches its peak of 1800 W at pressures close to 80 bar, indicating a more efficient operating range for the gas cooler. From this point onward, the heat transfer rate drops again to 1500 W near 85 bar, followed by a decreasing stabilization toward the end of the studied pressure range. This behavior suggests the existence of an optimal pressure in the gas cooler, around 80 bar, where heat transfer is maximized.

The curve of the heat transfer rate absorbed by the primary fluid in the evaporator, shown in Figure 8, follows a trend similar to that of Figure 7, with an initial drop from 1420 W to 1150 W. From 76 bar onward, there is also a progressive increase until it reaches a peak of 1250 W, again near 80 bar, as observed in the gas cooler. After this point, the cooling capacity decreases again, reaching 1000 W at pressures close to 85 bar, and continues to decline gradually.

The next parameter to be analyzed is the system's Coefficient of Performance, shown in Figure 9.

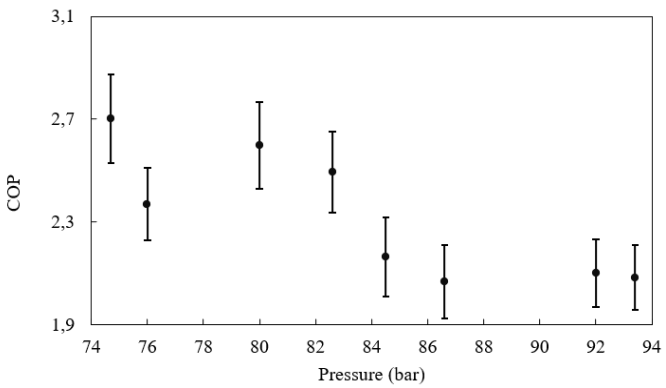

Figure 9. COP for the system operating as a refrigerator.

As seen in Figure 8, the heat transfer rate from the water to the fluid in the evaporator undergoes an initial drop from 1420 W to 1150 W at pressures around 76 bar. It then increases gradually, reaching a peak of 1250 W, near 80 bar — a pattern that coincides with the COP curve in Figure 9, where the highest values, approximately 2.7, are observed. This indicates that the increase in the system's cooling capacity directly contributes to the improvement of its efficiency within this operating range. However, as shown in Eq. 3 and 4, the COP also accounts for the amount of energy supplied to the compressor. Therefore, it can be inferred that the 80 bar range not only enhances heat exchange between the primary and secondary fluids, but does so efficiently compared to other operating points, offering a favorable ratio between cooling output and energy consumption. For pressures above 82 bar, however, the COP curve shows a continuous decline, indicating that the increased compressor work at higher pressures outweighs the heat transfer rates in the evaporator, leading to reduced system efficiency.

According to Chen and Gu (2005), an increase in the gas cooler pressure causes a decrease in the enthalpy value of CO_2 at the evaporator inlet, which causes an increase in the COP, according to Eq. 4. For higher pressures, the effect of pressure on this enthalpy is smaller, while the compressor power continues to increase, resulting in a trade-off between cooling capacity and compressor work. This, combined with the effect of the CO_2 mass flow rate on the cooling capacity, helps to explain the COP behavior observed in Figure 9.

It is worth noting that although the system shows good COP and cooling capacity values at pressures near the critical point for CO_2, such as 74 bar, operating in this region may not be feasible or preferable in practice. At pressures below 74 bar, the system would begin to operate subcritically, where heat is rejected via condensation. This process requires the CO_2 temperature to be higher than that of the secondary fluid. In many practical scenarios, the secondary fluid's temperature may not be lower than the CO_2 condensation temperature, which can fall below 25°C in a subcritical cycle. This would make heat rejection in the condenser impossible, rendering this pressure range unsuitable for applications like the one in this study.

To contextualize the results obtained in this experiment within the current scenario, a comparison was made with the work of Bellos and Tzivanidis (2019), where the authors proposed a comparison of different configurations of refrigeration systems using CO_2 via computational simulation. Thus, the system with a configuration similar to that of the present study, named by the authors as the "Reference system" – comprising a compressor, an expansion valve, a gas cooler and an evaporator – presented a COP range from 0.42 to 2.64, depending on the operating conditions. These results align directly with those obtained experimentally in this study, with a maximum COP of approximately 2.7 at pressures near 80 bar. Therefore, this similarity serves as a validation of the proposed setup, confirming the feasibility of using this small-scale system operating with CO_2 in a transcritical cycle.

It is important to mention that, although it is not the focus of this work, the efficiency of the machine operating as a heat pump can also be calculated. For this, it is only necessary to consider that the useful heat from Eqs. 3 and 4 is no longer the heat transfer rate at the evaporator, but rather the one observed at the gas cooler, as shown in Figure 7. Since the behavior of the heat transfer rate curves in both heat exchangers is similar, the system's COP curve as a heat pump would also be like that shown in Figure 9, but with higher values, given that the compressor work remains the same.

Finally, using the mass flow rates and the fluid properties obtained from the sensor data, it was possible to calculate the volumetric efficiency of the compressor. The results are shown in Figure 10.

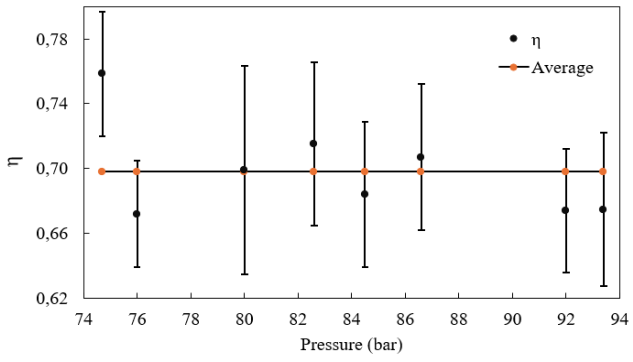

Figure 10. Volumetric efficiency of the compressor for each test.

Analyzing this curve, it can be observed, as shown in Figure 6, a non-linear behavior. Initially, there is a sharp drop in the compressor efficiency, from around 75% to values close to 67%, which can be explained by the change in mass flow caused by the electronic expansion valve. After that, the efficiency increases to a peak of 71% at pressures near 82 bar. Again, a favorable point is observed in this pressure range, as also noted in the analyses of heat exchange rates and COP. Similar to the mass flow, the volumetric efficiency curve decreases from 82.5 bar to 84 bar, then rises again up to pressures of 86 bar. From this pressure onward, compression becomes less efficient, and the curve undergoes a continuous and gradual decline. Overall, the compressor efficiency was around 70%, which, compared to other systems, can be considered an acceptable value for this type of application.

4. CONCLUSION

This work consists of the experimental characterization of a small-scale refrigeration system operating with CO_2 in a transcritical cycle focused on the influence of gas cooler pressure variation on the system's performance parameters. The results showed a nonlinear response in the parameters of CO_2 mass flow rate, heat transferred in the heat exchangers, COP, and finally, the compressor's volumetric efficiency. Within this response, the pressure range of 80 bar emerged as the system's optimal operating pressure, where the cooling capacity (1250 W), heat transfer rate in the gas cooler (1800 W), and COP (2.7) reached their maximum values. Thus, this point represents the best balance between the amount of heat exchanged and the compressor work, highlighting the sensitivity of transcritical systems to gas cooler pressure variations.

The system's ability to control temperature, pressure, and flow rate resulted in a robust machine, supporting the validation of the feasibility of using refrigeration systems with this configuration in small-scale applications, such as domestic refrigeration units. In this way, this study provides operational parameters to boost compact CO_2 refrigeration systems, replacing synthetic fluids and accelerating the transition to renewable technologies with low environmental impact.

5. ACKNOWLEDGMENT

The authors would like to thank FAPEMIG (Fundação de Amparo a Pesquisa do Estado de Minas Gerais) for its financial support and the Office of the Dean for Research at the Universidade Federal de Minas Gerais for its support during the writing of this manuscript. This study was also financed in part by the Coordenação de Aperfeiçoamento de Pessoal de Nível Superior - Brasil (CAPES) - Finance Code 001.

6. REFERENCES

Cao, Feng, Yulong Song, e Mingjia Li. 2019. “Review on development of air source transcritical CO2 heat pump systems using direct-heated type and recirculating-heated type”. *International Journal of Refrigeration* 104:455–75. doi:10.1016/j.ijrefrig.2018.12.023.

Chen, Ying, e Junjie Gu. 2005. “The Optimum High Pressure for CO2 Transcritical Refrigeration Systems with Internal Heat Exchangers”. *International Journal of Refrigeration* 28(8):1238–49. doi:10.1016/j.ijrefrig.2005.08.009.

Climate Reanalyzer. 2024. “Climate Change Institute. Available from: https://climatereanalyzer.org/wx/todays-weather/?var_id=t2&ortho=1&wt=2”.

Deng, Sensen, Dong Wang, Yuehong Lu, e Baomin Dai. 2025. “Novel optimal high pressure determination method for CO2 air source heat pump water heater: Experimental study and methodology development”. *Applied Thermal Engineering* 258(PA):124564. doi:10.1016/j.applthermaleng.2024.124564.

Guruchethan, A. M., Y. Siva Kumar Reddy, M. P. Maiya, e Armin Hafner. 2023. “Performance evaluation of absorption cooling assisted transcritical CO2 refrigeration systems”. *International Journal of Refrigeration* 155(September):362–74. doi:10.1016/j.ijrefrig.2023.09.012.

Intergovernmental Panel on Climate Change (IPCC). 2007. *Climate Change 2007: The Physical Science Basis – Summary for Policymakers. Contribution of Working Group I to the Fourth Assessment Report*. Geneva, Switzerland: World Meteorological Organization (WMO) and United Nations Environment Programme (UNEP), IPCC Secretariat.

Lorentzen, Gustav. 1994. “Revival of carbon dioxide as a refrigerant”. *H and V Engineer* 66(721):9–14.

Lykas, Panagiotis, Nikolaos Georgousis, Evangelos Bellos, e Christos Tzivanidis. 2022. “Investigation and optimization of a CO2-based polygeneration unit for supermarkets”. *Applied Energy* 311(February):118717. doi:10.1016/j.apenergy.2022.118717.

Martins, Erick, Guilherme Ramiro, e Antônio Maia. 2024. “Desenvolvimento de um mecanismo de expansão eletrônico para um sistema de refrigeração de pequeno porte operando com CO2 em um ciclo transcrítico.” 2:1–10. doi:10.26678/abcm.conem2024.con24-1126.

Oruç, Vedat, Atilla G. Devecioğlu, e Derviş B. İlhan. 2024. “Retrofit of an internal heat exchanger in a R404A refrigeration system using R452A: Experimental assessment on the energy efficiency and CO2 emissions”. *Next Energy* 3(January):100107. doi:10.1016/j.nxener.2024.100107.

Song, Yulong, Ce Cui, Xiang Yin, e Feng Cao. 2022. “Advanced development and application of transcritical CO2 refrigeration and heat pump technology—A review”. *Energy Reports* 8:7840–69. doi:10.1016/j.egyr.2022.05.233.

United Nations (UN). 1997. *Kyoto Protocol to the United Nations Framework Convention On Climate Change*. New York, NY, USA: United Nations.

Yadav, Saurabh, Jie Liu, e Sung Chul Kim. 2022. “A comprehensive study on 21st-century refrigerants - R290 and R1234yf: A review”. *International Journal of Heat and Mass Transfer* 182:121947. doi:10.1016/j.ijheatmasstransfer.2021.121947.

7. RESPONSIBILITY NOTICE

The authors are the only responsible for the printed material included in this paper.